

The absorption spectra of thin films of ternary compounds in the RbI–PbI₂ system

O. N. Yunakova, V. K. Miloslavskii, E. N. Kovalenko, and E. V. Ksenofontova

Citation: *Low Temp. Phys.* **38**, 943 (2012); doi: 10.1063/1.4758777

View online: <http://dx.doi.org/10.1063/1.4758777>

View Table of Contents: <http://ltp.aip.org/resource/1/LTPHEG/v38/i10>

Published by the [American Institute of Physics](#).

Related Articles

Optical properties of Mg-doped VO₂: Absorption measurements and hybrid functional calculations
Appl. Phys. Lett. **101**, 201902 (2012)

Electronic and optical properties of vacancy-doped WS₂ monolayers
AIP Advances **2**, 042141 (2012)

Effect of N₂ dielectric barrier discharge treatment on the composition of very thin SiO₂-like films deposited from hexamethyldisiloxane at atmospheric pressure
Appl. Phys. Lett. **101**, 194104 (2012)

Ultrafast nonlinear optical responses of bismuth doped silicon-rich silica films
Appl. Phys. Lett. **101**, 191106 (2012)

Optical and structural properties of SiO_x films grown by molecular beam deposition: Effect of the Si concentration and annealing temperature
J. Appl. Phys. **112**, 094316 (2012)

Additional information on Low Temp. Phys.

Journal Homepage: <http://ltp.aip.org/>

Journal Information: http://ltp.aip.org/about/about_the_journal

Top downloads: http://ltp.aip.org/features/most_downloaded

Information for Authors: <http://ltp.aip.org/authors>

ADVERTISEMENT

**AIP**Advances

Submit Now

**Explore AIP's new
open-access journal**

- **Article-level metrics
now available**
- **Join the conversation!
Rate & comment on articles**

LOW-DIMENSIONAL AND DISORDERED SYSTEMS

The absorption spectra of thin films of ternary compounds in the RbI–PbI₂ systemO. N. Yunakova^{a)} and V. K. Miloslavskii*V.N. Karazin Kharkiv National University, pl. Svobody, 4, Kharkov 61077, Ukraine*

E. N. Kovalenko

Kharkiv National University of Radio Electronics, Lenin Ave., 14, Kharkov 61166, Ukraine

E. V. Ksenofontova

V.N. Karazin Kharkiv National University, pl. Svobody, 4, Kharkov 61077, Ukraine

(Submitted January 16, 2012; revised February 24, 2012)

Fiz. Nizk. Temp. **38**, 1191–1196 (October 2012)

Formation of compounds RbPbI₃ and Rb₄PbI₆ in the RbI–PbI₂ system is revealed, and their absorption spectra are investigated in an energy interval of 2–6 eV and at temperatures from 90 to 500 K. It is established that the low-frequency exciton excitations are localized in PbI₆^{4–} structural elements of the crystal lattice, they are classified as excitons of intermediate coupling and are of a three-dimensional character in RbPbI₃ and a quasi-two-dimensional one in Rb₄PbI₆.

© 2012 American Institute of Physics. [<http://dx.doi.org/10.1063/1.4758777>]

According to previous thermographic investigations,¹ compounds RbPbI₃ and Rb₉PbI₁₁ are formed in the RbI–PbI₂ system, while ternary compounds CsPbI₃ and Cs₄PbI₆ form in the isomorphous system CsI–PbI₂. Compounds RbPbI₃ and CsPbI₃ are isostructural, and at room temperature they crystallize in the orthorhombic perovskite-like lattice with four molecules per unit cell, and similar parameters: $a = 10.27 \text{ \AA}$; $a = 10.46 \text{ \AA}$, $b = 17.38 \text{ \AA}$; $b = 17.78 \text{ \AA}$, $c = 4.77 \text{ \AA}$; $c = 4.8 \text{ \AA}$ (space group P_{nma}) in RbPbI₃ and CsPbI₃ respectively.^{2–4} Structural elements of the RbPbI₃ and CsPbI₃ lattices are double chains consisting of (PbI₆)^{4–} octahedra and oriented along the short axis c . Unlike CsPbI₃, for which the phase transition to the monoclinic phase has been determined to take place in the temperature range between 563 K and 602 K³ (to the cubic phase with $a = 6.29 \text{ \AA}$ according to a more recent study⁴), in RbPbI₃ no phase transition has been detected.⁴

Early studies of the reflection spectra of single crystals RbPbI₃ and CsPbI₃ (Ref. 5) established their similarity in the measured spectral range (2.9–3.2 eV). However, measurements in Ref. 5 were conducted in a very narrow spectral range, which did not include the absorption range of the second complex compound of the RbI–PbI₂ and CsI–PbI₂ systems, and do not give complete information about the electronic spectrum of the compounds and the monophase character of the crystals. While the absorption spectrum of CsPbI₃ has been studied by many authors,^{5–9} only one study is known regarding the spectrum of RbPbI₃,⁵ which, apparently, as is the case for CsPbI₃,^{6–9} is due to the difficulty in obtaining single-phase films of RbPbI₃ without admixture of a second compound, which is formed in the RbI–PbI₂ system.

The second ternary compound, Rb₉PbI₁₁, which forms in the (RbI) _{x} (PbI₂)_{1– x} system for large values of x according to Ref. 1, has not been studied.

The method developed for obtaining single-phase films of ternary compounds in the (RbI) _{x} (PbI₂)_{1– x} system allowed to obtain thin films of compounds and examine their absorption

spectra in a wide spectral range of 2–6 eV and temperatures from 90 K to 520 K.

Experiment

Thin films of RbPbI₃ were prepared by vacuum evaporation of a mixture of pure RbI and PbI₂ powders in stoichiometric amounts onto heated quartz substrates. The mixture of powders is first melted under a screen placed between the evaporator and the substrate, and then the melt is evaporated onto the substrate. The substrate temperature was varied from 373 to 403 K. When the substrate temperature is $T_{\text{sub}} = 393 \text{ K}$ we get monophasic RbPbI₃ films with the characteristic for the substance spectrum, similar to that of CsPbI₃,^{7–9} with an intense long-wavelength A^{I} -band at 2.975 eV (90 K) at the absorption edge. In the spectrum of thin films prepared at a lower substrate temperature $T_{\text{sub}} \approx 353 \text{ K}$, except for the A^{I} -band inherent to RbPbI₃, a higher-frequency A^{II} -band appears, corresponding, apparently, to the second triple junction (Fig. 1, curve 1). A similar situation was observed for the compounds of the CsI–PbI₂ system,^{6–9} in which at low substrate temperatures ($T_{\text{sub}} \leq 353 \text{ K}$) two-phase films were obtained (Fig. 1, curve 3), which after annealing for several hours at a temperature above 400 K transitioned into single-phase films with a spectrum characteristic for Cs₄PbI₆ (Fig. 1, curve 4).⁹ The spectra of two-phase films produced in CsI–PbI₂ and RbI–PbI₂ systems are similar structurally and in the position of the main absorption bands (Fig. 1). After annealing the two-phase films (RbI)_{0.5}(PbI₂)_{0.5} for two hours at a high temperature $T_{\text{ann}} \sim 673 \text{ K}$ their absorption spectrum changed (Fig. 1, curve 2): in terms of the structure of the spectrum and position of the main absorption bands it became similar to the spectrum of Cs₄PbI₆ (Fig. 1). Apparently, in the (RbI) _{x} (PbI₂)_{1– x} system for large values of x a compound of the same molar composition as (CsI) _{x} (PbI₂)_{1– x} is formed. It should be noted that upon evaporation from the melt two-phase films are usually obtained that

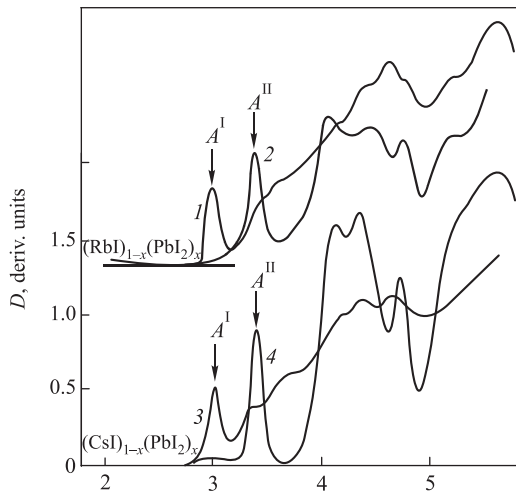


FIG. 1. Absorption spectra of two-phase films $(\text{RbI})_{1-x}(\text{PbI}_2)_x$ and $(\text{CsI})_{1-x}(\text{PbI}_2)_x$ ($x=0.5$, $T=90$ K) prior to annealing (1, 3) and after annealing ($T_{\text{ann}}=673$ K (2), $T_{\text{ann}}=400$ K (4)).

transition into Rb_4PbI_6 at high annealing temperature, but often after this light scattering appears in the films due to the very high annealing temperature. Optically smooth indispersive Rb_4PbI_6 films are obtained by evaporation of the molten mixture of RbI and PbI_2 powders of stoichiometric amounts onto quartz substrates heated up to $T_{\text{sub}} \geq 433$ K, followed by annealing the samples for 2 h at the same temperature. The synthesis of RbPbI_3 films without admixture of Rb_4PbI_6 requires careful selection of the substrate temperature and the rate of evaporation of the melt and is a great challenge.

Phase composition of the films was monitored via absorption spectra measured at 90 K. Such monitoring is possible because of the significant differences in the spectral position of long-wavelength exciton bands in RbPbI_3 (2.975 eV), Rb_4PbI_6 (3.41 eV), PbI_2 (2.5 eV), and RbI (5.7 eV).

Absorption spectra of thin films were measured using a spectrophotometer SF-46 in the spectral region between 2 and 6 eV in the temperature range of 90–500 K. For the measurement, films 80–120 nm thick were used. The spectral width of the gap in the region of the most narrow long-wavelength exciton bands is 0.02 eV, i.e., much smaller than the half-width of the exciton bands ($\Gamma \sim 0.1$ eV at $T=90$ K).

Parameters of the long-wavelength exciton bands (the position of E_m , the half-width Γ , and $\varepsilon_{2m} = \varepsilon_2(E_m)$, which is the value of the imaginary part of the dielectric constant at the band maximum) were determined by the method described in Ref. 10, by fitting the exciton band to a single-oscillator symmetrical circuit, which is essentially a combination of Lorentzian and Gaussian circuits. The exciton band parameters (E_m , Γ , and ε_{2m}) were selected in such a way that on the long-wavelength side the calculated and the experimental circuits were in good agreement.

Absorption spectra of RbPbI_3 and Rb_4PbI_6 thin films

In the absorption spectrum of the RbPbI_3 thin film an intense long-wavelength A_1^I -band is observed at 2.975 eV (90 K) (Fig. 2(a)), shorter-wavelength bands C_1^I , C_2^I , C_3^I , and D^I (the spectral position of the bands is given in Table 1) are located amid interband absorption. In Rb_4PbI_6 the absorption edge is shifted towards the lower wavelength region of the

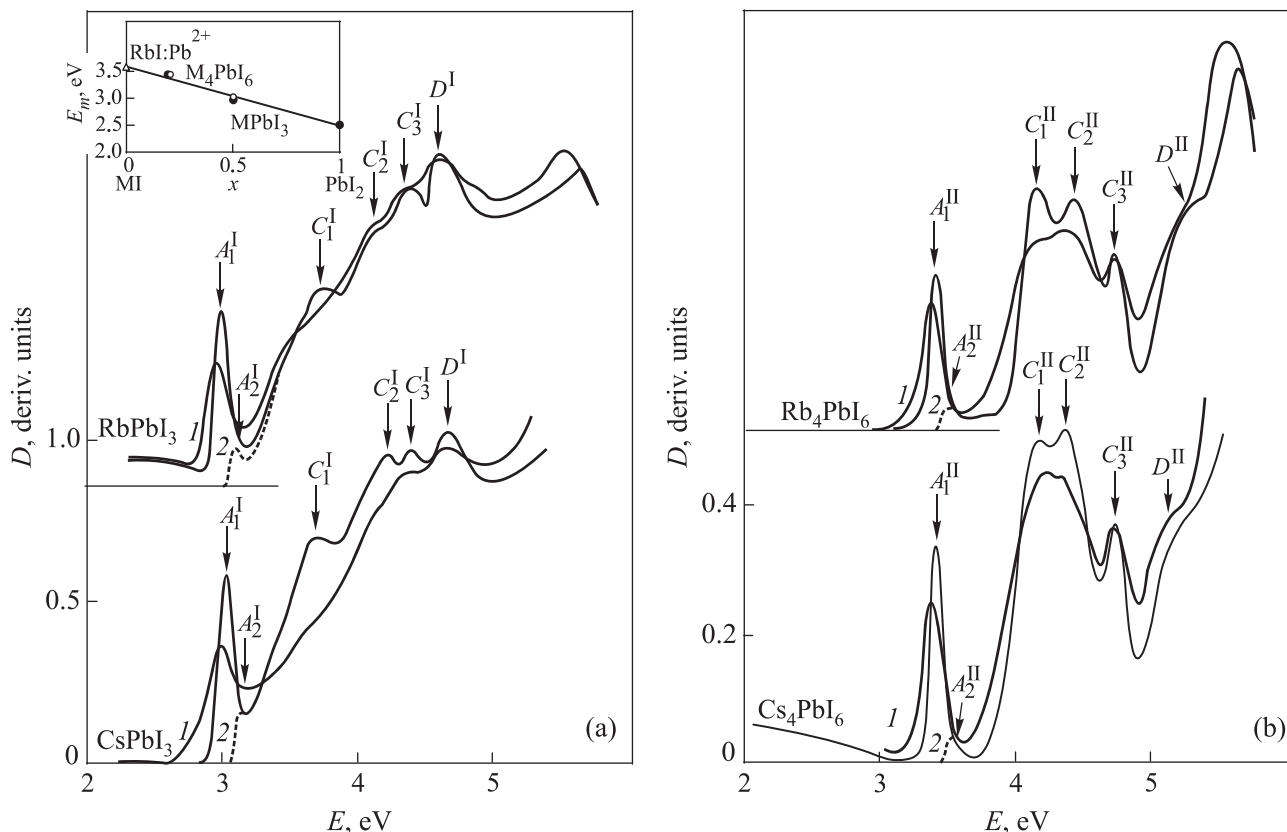


FIG. 2. The absorption spectra of RbPbI_3 , CsPbI_3 (a) and Rb_4PbI_6 , Cs_4PbI_6 (b) thin films at various temperatures T , K: 290 (1), 90 (2), dashed line—the edge of absorption after separating the A_1 -band by a symmetrical contour. The inset shows the concentration dependence of the spectral position of E_m in the line of compounds PbI_2 , MPbI_3 , M_4PbI_6 ($M = \text{Cs, Rb}$), $M = \text{Cs}$ (O), $M = \text{Rb}$ (●), (Δ)—spectral position of Pb^{2+} in RbI .

TABLE 1. The spectral position of the absorption bands, the exciton binding energy R_{ex} , and the band gap E_g in these compounds.

Compound	E_{A1} , eV	E_{A2} , eV	E_{C1} , eV	E_{C2} , eV	E_{C3} , eV	E_D , eV	R_{ex} , eV	E_g , eV
CsPbI ₃ [9]	3.013	3.131	3.69	4.22	4.4	4.461	0.157	3.17
RbPbI ₃	2.975	3.1	3.73	4.105	4.4	4.63	0.167	3.142
Cs ₄ PbI ₆ [9]	3.41	3.522	4.19	4.36	4.73	5.2	0.149	3.56
Rb ₄ PbI ₆	3.41	3.512	4.1	4.43	4.73	5.28	0.133	3.543
RbI:PbI ₂ [11]	3.543			4.5		4.87		

spectrum by 0.44 eV with respect to RbPbI₃ (Fig. 2(b)), the long-wavelength A_1^{II} -band is located at 3.41 eV (90 K), and in the low-wavelength region intensive C_1^{II} -, C_2^{II} -, and D^{II} bands are observed (see E_m in Table 1).

With increasing temperature, the A-, C-, and D-bands in the absorption spectra of both compounds are shifted to longer wavelengths, broadened, and weakened due to the exciton-phonon interaction (EPI), which indicates their relationship with the exciton excitations.

After the separation of the A_1^{I} - and A_1^{II} -bands by a symmetric contour on the long-wavelength side of C_1^{I} - and C_1^{II} —in RbPbI₃ and Rb₄PbI₆ weak A_2^{I} - and A_2^{II} -bands are observed, which we attribute to the excitation of 2s-excitons ($n = 2$). Considering that bands A_1^{I} (A_1^{II}) and A_2^{I} (A_2^{II}) refer to the exciton series with A_1^{I} (A_1^{II}) as the dominant band, based on their spectral position in the Wannier-Mott approximation of excitons we estimate the exciton binding energy $R_{ex} = 4/3(E_{A2} - E_{A1}) = 0.153$ eV, $R_{ex} = 0.133$ eV and the width of the band gap $E_g = E_{A1} + R_{ex}$, equal to 3.14 eV in RbPbI₃ and 3.54 eV in Rb₄PbI₆.

For the interpretation of absorption spectra of RbPbI₃ and Rb₄PbI₆ thin films we compare them with the spectra of the previously studied compounds CsPbI₃ and Cs₄PbI₆ (Fig. 2).⁹ As seen in Fig. 2, the absorption spectra of CsPbI₃ and RbPbI₃, Cs₄PbI₆ and Rb₄PbI₆ are similar in structure and with respect to the position of absorption bands (see Table 1), indicating the localization of excitons in the cation sublattice of the compounds, which contains lead ions. Also in favor of this localization, we observe a linear dependence of the spectral position of the long-wavelength exciton bands on the molar concentration x of PbI₂ in a line of compounds PbI₂, RbPbI₃, Rb₄PbI₆, PbI₂, CsPbI₃, Cs₄PbI₆, converging for $x \rightarrow 0$ to $E = 3.6$ eV, which is significantly less than the spectral position of admixture bands of Pb²⁺ in RbI¹¹ (Fig. 2, inset). According to the concept developed for multi-component compounds and solid solutions,¹² in the case of localization of excitons in the sublattice of one of the components, with its decrease the low-frequency bands converge to the spectral position of the impurity bands of the metal in the lattice of the second component.

With the localization of excitons in PbI₂ sublattice of compounds RbPbI₃ and Rb₄PbI₆ the top of the valence band in them, as in PbI₂,¹³ is formed by Pb 6s-states mixed with some I 5p-states, and the conduction band—by Pb 6p-states, and excitons, as in PbI₂,¹³ are cationic in nature. Therefore, absorption spectra of RbPbI₃ and Rb₄PbI₆, like the spectra of CsPbI₃, Cs₄PbI₆,⁹ and PbI₂,¹³ should be treated on the basis of electronic transitions in the (PbI₆)⁴⁻ octahedra, the structural elements of the crystal lattices of the compounds,²⁻⁴ similarly to the spectra of Pb²⁺ impurity ions in alkali-halide crystals.¹¹ For the Pb²⁺ impurity ions

in a lattice of D_{3d} symmetry the following transitions are characteristic: $A-^1A_{1g}$ band $\rightarrow ^3T_{1u}$ ($^1S_0 \rightarrow ^3P_1$ in the free Pb²⁺ ion), $B-^1A_{1g}$ band $\rightarrow ^3T_{2u}$ or 3E_u ($^1S_0 \rightarrow ^3P_2$), $C-^1A_{1g}$ band $\rightarrow ^1T_{1u}$ ($^1S_0 \rightarrow ^1P_1$).¹¹ The sharp long-wavelength edge and the high intensity of A- and C-bands in the RbPbI₃ and Rb₄PbI₆ spectra indicate their relation to direct allowed transitions in the (PbI₆)⁴⁻ structural elements of the lattices of the compounds and, as in RbI:Pb²⁺, they apparently correspond to the transitions $^1A_{1g} \rightarrow ^3T_{1u}$ (the A-band) and $^1A_{1g} \rightarrow ^1T_{1u}$ (the C-bands). The B-band corresponding to the forbidden transition in Pb²⁺ impurity centers does not appear in our spectra.

Temperature dependence of the long-wavelength parameters of exciton absorption bands in RbPbI₃ and Rb₄PbI₆

The absorption spectra of RbPbI₃ and Rb₄PbI₆ thin films in the long-wavelength exciton band (2.4–3.7 eV) were measured in the temperature range from 90 to 500 K.

With increasing temperature the A_1^{I} band in RbPbI₃ shifts linearly to longer wavelengths with dE_m/dT

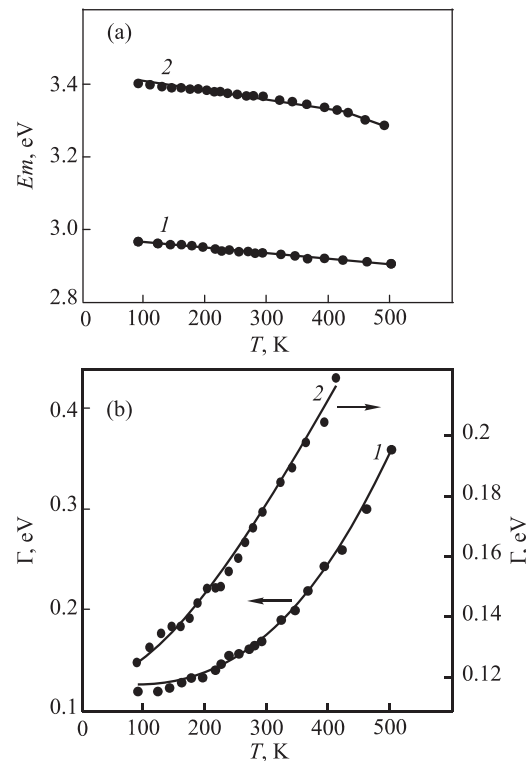


FIG. 3. Temperature dependence of the spectral position $E_m(T)$ (a) and half-width $\Gamma(T)$ (b) of the long-wavelength exciton band A_1^{I} in RbPbI₃ (1) ($t = 80$ nm) and A_1^{II} -band in Rb₄PbI₆ (2) ($t = 120$ nm); dots represent experimental data, solid lines (b) were calculated from Eq. (1) for $d = 3$ (1) and $d = 2$ (2).

$dT = -1.73 \cdot 10^{-4}$ eV/K (Fig. 3(a)), close to the value of $dE_m/dT = -1.6 \cdot 10^{-4}$ eV/K in PbI_2 thin films.¹⁴ With respect to the order of magnitude, such a shift is typical for most ionic crystals, including the compounds studied here. In ionic crystals the interaction of excitons with longitudinal optical (LO) phonons and the greatest temperature-dependent changes of the exciton band parameters occur at $\hbar\omega_{LO} \leq kT$. Unknown values of $\hbar\omega_{LO}$ in RbPbI_3 and Rb_4PbI_6 can be estimated from the known values of $\hbar\omega_{LO} = 13.7$ meV in PbI_2 ,¹⁵ and $\hbar\omega_{LO} = 13.2$ meV in RbI .¹⁶ Given the molar composition of the compounds, in RbPbI_3 $\hbar\omega_{LO} \sim 13.45$ meV, and in Rb_4PbI_6 $\hbar\omega_{LO} \sim 13.3$ meV.

Temperature dependence of the half-width of the A_1^1 -band in RbPbI_3 $\Gamma(T)$ is shown in Fig. 3(b). The dependence $\Gamma(T)$ for excitons of different dimension d ($d=1, 2, 3$) according to theory¹⁷ is defined as

$$\Gamma(T) \approx \left[\frac{\pi D^2}{\gamma(d/2)(2\pi B)^{d/2}} \right]^{\frac{2}{4-d}}, \quad (1)$$

where $\gamma(d/2)$ is the gamma function, B is the exciton band width, $D^2 = 0.5C^2 \hbar\omega_{LO} \text{cth}(\hbar\omega_{LO}/kT)$, and $C^2/2$ is the energy of lattice relaxation in the exciton. The contribution of the residual broadening $\Gamma(0)$ to the total half-width of the exciton band Γ due to the lattice defects should also be taken into account. In RbPbI_3 the exciton band A_1^1 has a Gaussian shape in the entire investigated temperature range. In this case, the total half-width of Γ is defined as

$$\Gamma = [\Gamma^2(0) + \Gamma^2(T)]^{1/2}, \quad (2)$$

where $\Gamma(T)$ obeys Eq. (1) with an unknown factor A , independent of T .

Treatment of the experimental dependence $\Gamma(T)$ using Eq. (1) for different values of d gives the best agreement of the calculation with experiment for $d=3$. In this case

$$\Gamma(T) = A \text{cth}^2(\hbar\omega_{LO}/kT) \quad (3)$$

and the dependence $\Gamma(T)$ in the coordinates Γ^2 from $\text{cth}^4(\hbar\omega_{LO}/kT)$ is linear. Treatment of this relationship by least squares gives the values $\Gamma(0) = (0.126 \pm 0.004)$ eV and $A = (0.78 \pm 0.006) \cdot 10^{-2}$ eV. Calculated using Eqs. (2) and (3), temperature dependence $\Gamma(T)$ with the found values of $\Gamma(0)$ and A is in good agreement with the experimental one (Fig. 3(b)).

In Rb_4PbI_6 the temperature dependence of the spectral position $E_m(T)$ in the range of $90 \text{ K} \leq T \leq 440 \text{ K}$ is linear (Fig. 3(a)): $E_m(T) = E(0) - aT$, where $E(0) = (3.428 \pm 0.02)$ eV, $a = dE_m/dT = (2.27 \pm 0.06) \cdot 10^{-4}$ eV/K, and this is due to EPI. The temperature shift coefficient dE_m/dT is characteristic for ionic crystals in terms of order of magnitude. At $T > 430 \text{ K}$, a kink in the dependence $E_m(T)$ is observed with a stronger shift of the spectral position of the exciton band towards lower frequencies. Since in the temperature dependence of the half-width of $\Gamma(T)$ (Fig. 3(b)) near 430 K no features are observed, we do not link changes in $E_m(T)$ to a phase transition. At $T > 430 \text{ K}$ in Rb_4PbI_6 films there is slight light scattering, pointing to their destruction. In particular,

at high temperatures the film loses its continuity and transforms into an insula. This effect was observed, for example, in CuBr films. During high-temperature annealing of continuous films ($T_{\text{ann}} \sim 423 \text{ K}$) they turned into insulae,¹⁸ and their absorption spectrum changed significantly: spectrum inversion occurred in the region of exciton absorption, and near the exciton absorption bands rather intense transmittance bands appeared. In the initial stages such a process can lead to a significant change in the spectral position of the exciton bands. Perhaps the deviation of the spectral position of the long-wavelength exciton band in Rb_4PbI_6 at $T > 430 \text{ K}$ from a linear dependence is due to the above.

The shape of the exciton band A_1^1 is a Gaussian in the entire range of temperatures under investigation, and its total half-width Γ , with the contribution of residual broadening $\Gamma(0)$, is determined by Eq. (2). Treatment of the temperature dependence of the half-width Γ with Eq. (1) gives the best agreement with experiment for $d=2$ (Fig. 3(b)). In this case, $\Gamma(T) = A \text{cth}(\hbar\omega_{LO}/kT)$ and in the coordinates Γ^2 from $\text{cth}^2(\hbar\omega_{LO}/kT)$ the dependence is linear. Its treatment by the method of least squares gives the values $\Gamma(0) = (0.114 \pm 0.001)$ eV and $A = (0.34 \pm 0.003) \cdot 10^{-2}$ eV.

Thus, it follows from the analysis of the temperature dependence of $\Gamma(T)$ that the excitons in RbPbI_3 have three-dimensional character, and in Rb_4PbI_6 —two-dimensional. Perhaps the crystal structure of Rb_4PbI_6 is layered, which results in two-dimensional character of excitons, but to reach the final conclusion it is necessary to study the crystal structure.

The dispersion of the refractive index $n(\lambda)$ in RbPbI_3 and Rb_4PbI_6 thin films in the transparency region was determined by the interference method.¹⁹ The obtained dependences $n(\lambda)$ (Fig. 4) are well described by the Vempala single oscillator model²⁰

$$\varepsilon_1 = n^2 = 1 + \frac{E_d E_0}{E_0^2 - E^2}, \quad (4)$$

where $E = \hbar\omega$, E_0 and E_d —are the single oscillator model parameters. E_0 determines the spectral position of the effective

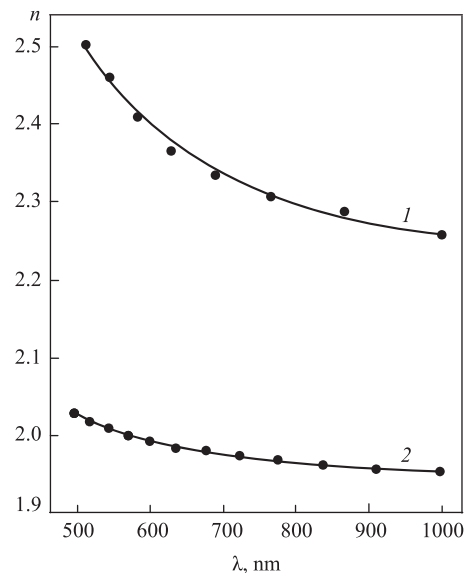


FIG. 4. Spectral dependence of the refractive index $n(\lambda)$ of RbPbI_3 (1) and Rb_4PbI_6 (2) thin films: dots represent experimental data, solid curves were calculated from Eq. (4).

oscillator associated with the interband optical transitions, the value of $E_0 > E_g$,¹⁹ and E_d is the dispersion energy, which characterizes the strength of interband transitions.

In coordinates $(n^2 - 1)^{-1} = f(E^2)$ the relationship (4) is linear. Treatment of the experimental data $n(\lambda)$ in these coordinates by least squares using the slope of the line allowed us to determine the value of $(E_0 E_d)^{-1} = 0.012 \pm 0.0002$ in RbPbI₃ thin films, $(E_0 E_d)^{-1} = 0.007 \pm 0.0002$ in Rb₄PbI₆ thin films, and the intersection with the ordinate axis value $E_0/E_d = 0.262 \pm 0.0015$; $E_0/E_d = 0.366 \pm 0.0015$ and, therefore, $E_0 = 4.63$ eV, $E_d = 17.83$ eV in RbPbI₃ thin films, and $E_0 = 7.22$ eV, $E_d = 19.72$ eV in Rb₄PbI₆ thin films. The calculated dependence of $n(\lambda)$ according to Eq. (4) (Fig. 4, solid line) with such values of E_0 and E_d is in good agreement with the experimental dependence $n(\lambda)$ (Fig. 4, point).

Approximating the dependence $n(\lambda)$ to the low energy limit according to Eq. (4) gives the value of the optical dielectric constant $\varepsilon_\infty = (1 + E_d/E_0) = 4.82$ in RbPbI₃ and $\varepsilon_\infty = 3.73$ in Rb₄PbI₆. The obtained values of ε_∞ were used to estimate the exciton radius in both compounds

$$a_{\text{ex}} = a_B \frac{R}{R_{\text{ex}} \varepsilon_{\text{eff}}}, \quad (5)$$

where $a_B = 0.529 \cdot 10^{-8}$ cm is the Bohr radius, $R = 13.6$ eV is the Rydberg constant, ε_{eff} is the effective dielectric permittivity, $\varepsilon_\infty < \varepsilon_{\text{eff}} < \varepsilon_0$, ε_0 is static dielectric permittivity, $R_{\text{ex}} = 0.153$ eV and $R_{\text{ex}} = 0.133$ eV are the defined above values of exciton binding energy in RbPbI₃ and Rb₄PbI₆, respectively. To estimate the radius of the exciton we used the lower limit of ε_{eff} , because in the low-frequency exciton band the main contribution to ε_{eff} is determined by the value of ε_∞ . The obtained values of the exciton radius $a_{\text{ex}} = 9.76$ Å in RbPbI₃ and $a_{\text{ex}} = 14.49$ Å in Rb₄PbI₆ allow us to attribute the exciton states in both compounds to intermediate coupling excitons.

Conclusion

Using the absorption spectra the formation of RbPbI₃ and Rb₄PbI₆ in the RbI-PbI₂ system has been determined. It is shown that in these compounds the long-wavelength exciton states are localized in the sublattices containing Pb²⁺

ions, surrounded by I⁻ ions, and refer to intermediate coupling excitons.

From the analysis of the temperature dependence of the exciton band parameters, the spectral position $E_m(T)$, and half-width $\Gamma(T)$ we conclude that there is no phase transition in RbPbI₃ in the studied temperature range.

The temperature dependence of $\Gamma(T)$ indicates a three-dimensional character of excitons in RbPbI₃ and a two-dimensional character in Rb₄PbI₆.

^{a)}Email: Olga.N.Yunakova@univer.kharkov.ua

¹I. N. Belyaev, E. A. Shurginov, and N. S. Kudryashov, *Zh. Neorg. Khim.* **17**, 281 (1972).

²V. H. J. Haupt, F. Huber, and H. Preut, *Z. Anorg. Allg. Chem.* **408**, 209 (1974).

³C. K. Møller, *Nature* **182**, 1436 (1958).

⁴D. M. Trots and S. V. Myagkota, *J. Phys. Chem. Solids* **69**, 2520 (2008).

⁵N. S. Pidzyrailo, A. S. Voloshinovskii, and S. V. Myagkota, *Opt. Spectra* **64**, 1187 (1988).

⁶F. Somma, M. Nikl, K. Nitsch, C. Giampaolo, A. R. Phani, and S. Santucci, *Revista Superficies y Vacio* **9**, 62 (1999).

⁷S. Kondo, A. Masaki, T. Saito, and H. Asada, *Solid State Commun.* **124**, 211 (2002).

⁸S. Kondo, K. Amaya, and T. Saito, *J. Phys.: Condens. Matter* **15**, 971 (2003).

⁹O. N. Yunakova, V. K. Miloslavskii, and E. N. Kovalenko, *Opt. Spectra* **112**, 90 (2012).

¹⁰O. N. Yunakova, V. K. Miloslavskii, and E. N. Kovalenko, *Opt. Spectra* **104**, 631 (2008).

¹¹K. Schmitt, *Phys. Status Solidi B* **135**, 389 (1986).

¹²Y. Onodera and Y. Toyasawa, *J. Phys. Soc. Jpn.* **22**, 833 (1967).

¹³I. Ch. Schlüter and M. Schlüter, *Phys. Rev. B* **9**, 1652 (1974).

¹⁴V. V. Mussil, V. K. Miloslavskii, and V. V. Karmazin, *Fiz. Tverd. Tela* **17**, 859 (1975).

¹⁵G. Lukovsky, R. M. White, J. A. Benda, W. Y. Liang, R. Zalle, and P. H. Schmidt, *Solid State Commun.* **18**, 811 (1976).

¹⁶*Excitons*, edited by E. I. Rashba (Nauka, Moscow, 1985).

¹⁷M. Schreiber and Y. Toyasawa, *J. Phys. Soc. Jpn.* **51**, 1528 (1982).

¹⁸V. K. Miloslavskii, A. I. Usoskin, and V. H. Thai, *Opt. Spectra* **59**, 87 (1985).

¹⁹S. P. Lyashenko and V. K. Miloslavskii, *Opt. Spectra* **16**, 151 (1964).

²⁰S. H. Wemple, *Phys. Rev. B* **7**, 3767 (1973).

Translated by D. K. Maraoulaite